

CORROSION INHIBITION OF 1018 C-STEEL BY SOME QUIONAZOLIN DERIVATIVES IN 2M HCL SOLUTION

Y.A. Elewady, H.A. Mostafa, S.A. Habouba and A.S. Fouda*

Chemistry Department, Faculty of Science, El-Mansoura University, El-Mansoura-35516, Egypt

*Corresponding author. Tel.: +02 050 2365730; fax: +02 050 2446254, email: asfouda@mans.edu.eg

Received: (2/4/2011)

ABSTRACT

Some quionazolin derivatives such as: 3-(4-chlorophenyl)-2-methylquinazolin-4(3H)-one (CMQ) and 2-methyl-3-(4-nitrophenyl) quinazolin-4(3H)-one (MNQ) were investigated as corrosion inhibitors for carbon steel in 2 M HCl solution. Electrochemical impedance spectroscopy (EIS), potentiodynamic polarization, electrochemical frequency modulation and weight loss methods were used to study the inhibition action at 30 °C. The corrosion of steel was controlled by a charge transfer process at the prevailing conditions. The electrochemical results showed that these compounds are efficient inhibitors for carbon steel and efficiency up to 93.8 % was obtained at 30 °C. The inhibition efficiency increases with inhibitor concentration. The adsorption of these compounds on carbon steel surface follows the Langmuir adsorption isotherm. The results show that the order of inhibition efficiency is CMQ > MNQ. Polarization curves indicate that investigated quionazolin derivatives are mixed-type inhibitors. The chemical and electrochemical methods gave similar results.

Keywords: Corrosion inhibitors, HCl, carbon steel, quionazolin derivatives.

INTRODUCTION

Carbon steel has been extensively used under different conditions in petroleum industries [Deyab, (2007)]. Aqueous solutions of acids are among the most corrosive media and are widely used in industries for pickling, acid cleaning of boilers, descaling and oil well [Abd El-Maksoud, and Fouda, (2005); Khaled, (2008); Machnikova *et al*, (2008); Ashassi-sorkhabi *et al*, (2004); Migahed, and Nasser, (2008)]. The main problem concerning carbon steel applications is its relatively low corrosion resistance in acidic solution. Several methods are used currently to prevent corrosion of carbon steel. One of such methods is the use of organic inhibitors [Avcı G., (2008); Pillali K.C., and Narayan R., (1985); Tadros, and Abdel-Naby, (1988); Bockris, and Yang,

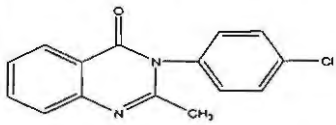
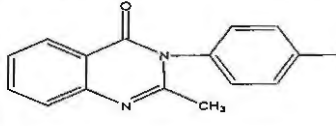
(1991); Effective inhibitors are heterocyclic Jovancicevic *et al*, (1989); Uhera , and Aramaki , (1991); Akust *et al*, (1982); Abdallah *et al*, (2006); Fouda *et al*, (2006); Fouda *et al*, (2006); Benali *et al*, (2007)]. compounds that have π bonds, heteroatoms such as sulphur, oxygen and nitrogen [Khalifa *et al*, (2003)]. Compounds containing both nitrogen and chloro atoms can provide excellent inhibition, compared with compounds containing only nitrogen or chloro atom [Abboud *et al*, (2007)]. Heterocyclic compounds such as quinazolin can provide excellent inhibition. These molecules depends mainly on certain physical properties of the inhibitor molecules such as functional groups, steric factors, electron density at the donor atom and electronic structure of the molecules [Khaled , (2003); Popova *et al*, (2004)]. Regarding the adsorption of the inhibitor on the metal surface, two types of interactions are responsible. One is physical adsorption which involves electrostatic force between ionic charges or dipoles of the adsorbed species and electric charge at metal/ solution interface. Other is chemical adsorption, which involves charge sharing or charge transfer from inhibitor molecules to the metal surface to form coordinated types of bonds [Noot and Al-Moubaraki , (2008)]. The selection of appropriate inhibitors mainly depends on the type of acid, its concentration, and temperature. In the present work, the inhibition characteristics of 3-(4-chlorophenyl)-2-methylquinazolin-4(3H)-one and 2-methyl-3-(4-nitrophenyl)quinazolin-4(3H)-one for carbon steel in HCl solution were investigated using chemical and electrochemical techniques.

EXPERIMENTAL

1. Chemicals and materials

Hydrochloric acid (37 %) ,ethyl alcohol and acetone were purchased from Algamhoria Company, Egypt, 3-(4-Chlorophenyl)-2-methylquinazolin-4(3H)-one (CMQ) and 2-Methyl-3-(4-nitrophenyl) quinazolin-4(3H)-one (MNQ) were synthesized as described before [Gao *et al*, (2007)] and the purity of the compounds was checked by TLC. The molecular structures and other details of these compounds are given in Table (1). Bidistilled water was used throughout all the experiments. The composition of 1018 carbon steel (weight %) is given in Table (2).

Table(1): Molecular structure, formula and molecular weight of investigated compounds

Inhibitor	Structure Formula	Mol. Formula & Mol.Weight
CMQ 3-(4-chlorophenyl)- 2-methylquinazolin- 4 (3H)-one		C ₁₅ H ₁₁ ClN ₂ O 270.056
MNQ 2-methyl-3-(4- nitrophenyl)quinazolin- 4 (3H)-one		C ₁₅ H ₁₁ N ₃ O ₃ 281.080

Table(2): Chemical composition of 1018 carbon steel

Chemical constituent	C	Mn	P	S	Fe
Composition (wt %)	0.14 - 0.20	0.6 - 0.9	0.04	0.05	rest

2. Methods:

2.1. Weight loss measurements :

Rectangular specimens of carbon steel with dimensions 2.1 cm x 2.0 cm x 0.2 cm were mechanically abrading with different grades of emery paper, degreased with acetone, rinsed with bidistilled water and dried between filter papers. After weighting accurately, the specimens were immersed in 100 ml of 2 M HCl with and without different concentration of inhibitors at 30 °C. After different immersion periods (each of 30 min till 180 min), the carbon steel samples were taken out, washed with bidistilled water, dried and weighted again.

The weight loss values are used to calculate the corrosion rate (R) in mmy⁻¹ by the relation:

$$R = (\text{weight loss in gram} \times 8.75 \times 10^4) / \text{DAT} \quad (1)$$

where D is carbon steel density in g cm⁻³, A is exposed area in cm², T is exposure time in hr.

The inhibition efficiency (%Y_w) and the degree of surface coverage (θ) were calculated from:

$$\%Y_w = [(R^* - R) / R^*] \times 100 \quad (2)$$

$$\theta = \frac{R^* - R}{R^*} \quad (3)$$

where R^* and R are the corrosion rates of carbon steel in the absence and in the presence of inhibitor, respectively.

2.2. Electrochemical measurements:

Electrochemical measurements were conducted in a conventional three electrodes thermostated cell assembly using an Gamry potentiostat/galvanostat/ZRA (model PCI4 750). A Pt foil and saturated calomel electrode (SCE) were used as counter and reference electrodes, respectively. The carbon steel electrodes were 1 cm x 1 cm and were welded from one side to a copper wire used for electrical connection. The electrodes were polished, degreased and rinsed as described in weight loss measurements. All experiments were carried out at temperature $(30 \pm 1^\circ\text{C})$. The potentiodynamic curves were recorded from -500 to 500 mV at a scan rate 5 mV S^{-1} after the steady state is reached (20 min) and the open circuit potential (OCP) was noted. The $Y_p\%$ and degree of surface coverage were calculated from the following equations:

$$Y_p\% = [1 - (i_{\text{corr}}^0 / i_{\text{corr}})] \times 100 \quad (4)$$

$$\theta = [1 - (i_{\text{corr}}^0 / i_{\text{corr}})] \quad (5)$$

where i_{corr}^0 and i_{corr} are the corrosion current densities of uninhibited and inhibited solution, respectively.

Electrochemical impedance spectroscopy (EIS) and electrochemical frequency modulation (EFM) experiments were carried out using the same instrument as before with a Gamry framework system based on ESA400. Gamry applications include software EIS300 for EIS measurements and EFM140 for EFM measurements, A computer was used for collecting data. Echem Analyst 5.5 Software was used for plotting, graphing and fitting data. EIS measurements were carried out in a frequency range of 100 kHz to 100 mHz with amplitude of 5 mV peak-to-peak using ac signals at respective corrosion potential. EFM carried out using two frequencies 2 and 5 Hz. The base frequency was 1 Hz. In this study, we use a perturbation signal with amplitude of 10 mV for both perturbation frequencies of 2 and 5 Hz.

RESULTS AND DISCUSSIONS

1. Weight loss measurements :

Figure (1): shows the weight loss-time curves for the corrosion of carbon steel in 2 M HCl in the absence and presence of different concentrations of CMQ. Similar curves for MNQ were obtained and are not shown. The data of Table (3) show that, the inhibition efficiency increases with the increase in inhibitor concentration from $0.05 \text{ m mol l}^{-1}$ to 2.5 m mol l^{-1} . The maximum inhibition efficiency was achieved at 2.5 m mol l^{-1} . The

lowest corrosion rate is obtained in the presence of MNQ, therefore $Y_w\%$ tends to decrease in the following order: CMQ > MNQ.

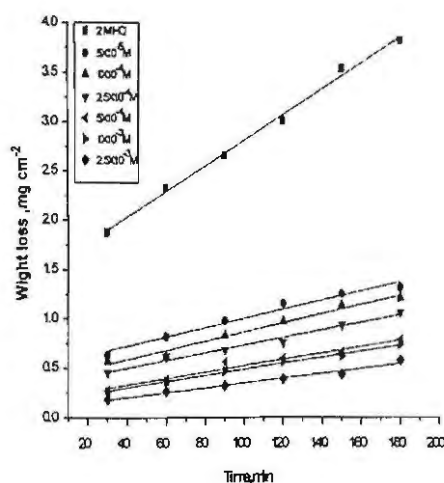


Fig (1): Weight loss-time curves of carbon steel in 2 M HCl in the absence and presence of different concentrations of CMQ at 30 °C.

Table(3): Data of weight loss measurements for carbon steel in 2 M HCl solution in the absence and presence of different concentrations of investigated compounds at 30 °C.

Compound	Conc., M	R (mg cm ⁻² min ⁻¹)	θ	% Y_w
Blank	0.00	0.0250	0.000	00.0
CMQ	5.0X10 ⁻⁵	0.0096	0.610	61.0
	1X10 ⁻⁴	0.0083	0.678	67.8
	2.5x10 ⁻⁴	0.0062	0.750	75.0
	5.0x10 ⁻⁴	0.0049	0.800	80.0
	1X10 ⁻³	0.0041	0.814	81.4
	2.5X10 ⁻³	0.0032	0.872	87.2
MNQ	5.0x10 ⁻⁵	0.0170	0.330	33.0
	1X10 ⁻⁴	0.0150	0.407	40.7
	2.5x10 ⁻⁴	0.0082	0.477	47.7
	5.0x10 ⁻⁴	0.0068	0.720	72.0
	1X10 ⁻³	0.0057	0.761	76.1
	2.5X10 ⁻³	0.0056	0.772	77.2

2. Electrochemical measurements :

2.1. Potentiodynamic polarization measurements

The potentiodynamic curves for carbon steel in 2 M HCl in the absence and presence of CMQ are shown in Fig.(2). Similar curves were obtained for MNQ (not shown). It is clear that; the investigated inhibitors affect the promoting retardation of anodic dissolution of carbon steel and cathodic hydrogen discharge reactions. Electrochemical parameters such as corrosion current density (i_{corr}), corrosion potential (E_{corr}), Tafel constants (β_a and β_c), degree of surface coverage (θ) and inhibition efficiency ($\%Y_p$) were calculated from Tafel plots and are given in Table (4). It is observed that the presence of inhibitor lowers i_{corr} . Maximum decrease in i_{corr} values was observed for CMQ indicating that this is the most effective corrosion inhibitor. It is also observed from Table 4 that E_{corr} values and Tafel slope constants do not change significantly in inhibited solution as compared to uninhibited solution. The investigated compounds do not shift the E_{corr} values significantly, suggesting that they behave as mixed type inhibitors [Ajmal *et al*, (1994)]. Both cathodic (β_c) and anodic Tafel lines (β_a) are parallel and are shifted to more negative and positive direction, respectively by adding inhibitors. This is indicating that the mechanism of the corrosion reaction does not change and the corrosion reaction is inhibited by simple adsorption mode [Bentiss *et al*, (2005)]. The irregular trends of β_a and β_c values indicate the involvement of more than one type of species adsorbed on the metal surface. The order of inhibition efficiency is as follows Table(4): CMQ > MNQ.

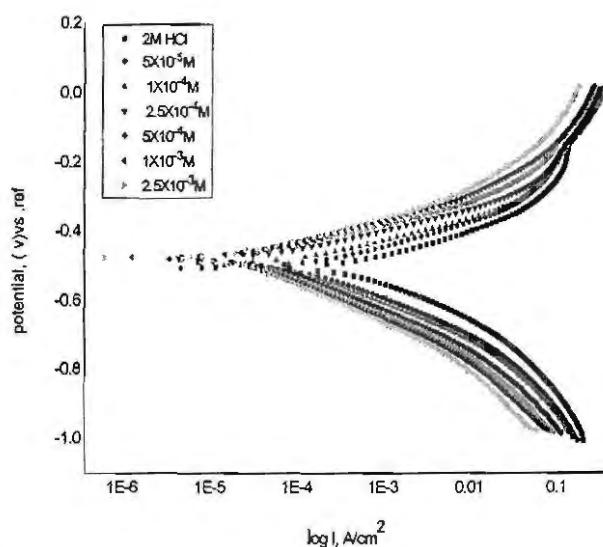


Fig. (2): Potentiodynamic polarization for corrosion of carbon steel in 2 M HCl in the absence and presence of different concentrations of CMQ at 30 °C.

Table (4): Potentiodynamic data of carbon steel in 2 M HCl and in the presence of different concentrations of inhibitors at 30 °C.

Compound	Conc., M	$-E_{\text{corr}}$, mVvs. SCE,	i_{corr} μA cm^{-2}	$-\beta_c$, mVdec^{-1}	β_a , mVdec^{-1}	θ	$Y_p\%$	R_p mmy^{-1}
Blank	0.0	499	359.0	98	69	0.000	00.0	164.1
CMQ	5×10^{-5}	504	139.0	101	69	0.618	61.8	71.0
	1×10^{-4}	492	76.6	102	60	0.787	78.7	38.9
	2.5×10^{-4}	479	41.1	107	59	0.886	88.6	20.8
	5×10^{-4}	476	29.8	108	62	0.917	91.7	15.3
	1×10^{-3}	476	23.7	110	67	0.930	93.0	12.2
	2.5×10^{-3}	474	21.1	116	71	0.938	93.8	11.0
MNQ	5×10^{-5}	494	141.0	103	71	0.590	59.0	71.2
	1×10^{-4}	503	127.0	93	55	0.610	61.0	75.2
	2.5×10^{-4}	499	120.0	101	60	0.665	66.5	63.5
	5×10^{-4}	490	73.6	108	61	0.795	79.5	37.7
	1×10^{-3}	487	46.6	109	65	0.870	87.0	24.8
	2.5×10^{-3}	471	31.2	117	69	0.913	91.3	16.9

2.2. Electrochemical impedance spectroscopy :

The EIS provides important mechanistic and kinetic information for an electrochemical system under investigation. Nyquist impedance plots obtained for the C-steel electrode at respective corrosion potentials after 15 min immersion in 2.0 M HCl in presence and absence of various concentrations of CMQ is shown in Fig.(3) (MNQ curves not shown). This diagram exhibits a single semi-circle shifted along the real impedance (Z_r). The Nyquist plots of CMQ do not yield perfect semicircles as expected from the theory of EIS, the impedance loops measured are depressed semi-circles with their centers below the real axis, where the kind of phenomenon is known as the "dispersing effect" as a result of frequency dispersion [El Achouri *et al*, (2001)] and

mass transport resistant [Khaled , (2003)] as well as electrode surface heterogeneity resulting from surface roughness, impurities, dislocations, grain boundaries, adsorption of inhibitors, formation of porous layers [Growcock F.B., and Jasinski J.H., (1989); Rammet, and Reinhart, (1987); Mehaute, and Grepy, (1983); Machnikova *et al*, (2008); Hsu, and Mansfeld, (2001)], etc .so one constant phase element (CPE) is substituted for the capacitive element, to explain the depression of the capacitance semi-circle, to give a more accurate fit.

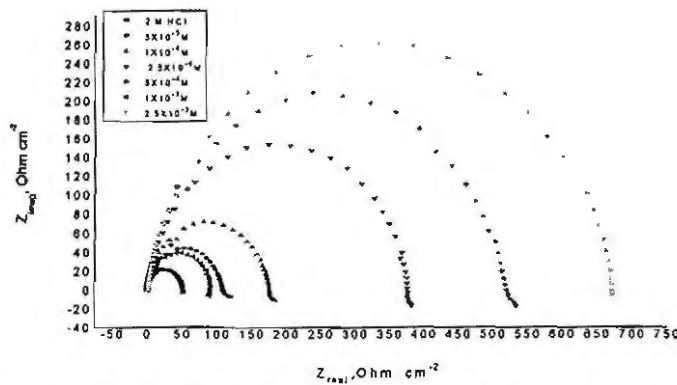


Fig. (3) :Nyquist plots for carbon steel in 2 M HCl at different concentrations of CMQ

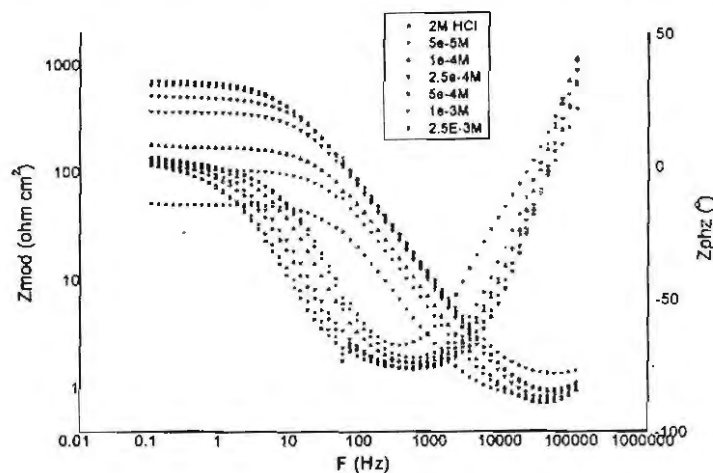


Fig (4): Bode plots for C-steel in 2 M HCl at different concentrations of CMQ
Impedance data are analyzed using the circuit in Fig.5; in which R_s represents the electrolyte resistance, R_{ct} represents the charge-transfer resistance and the constant phase element (CPE).

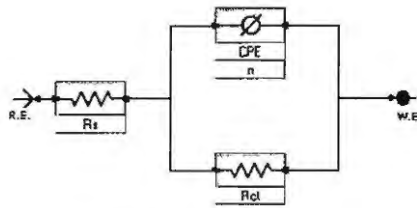


Fig (5): Equivalent circuit model used to fit the impedance spectra

According to Hsu and Mansfeld [Lebrini *et al*, (2007)] the correction of capacity to its real values is calculated from:

$$C_{dl} = Y_0 (\omega_{max})^{n-1} \quad (6)$$

where Y_0 is the CPE coefficient, ω_{max} is the frequency at which the imaginary part of impedance ($-Z_i$) has a maximum and n is the CPE exponent (phase shift).

The data obtained from fitted spectra are listed in Table 5. The degree of surface coverage (θ) is calculated from the EIS data by using following equation:

$$\theta = \frac{R_{ct} - R_{ct}^*}{R_{ct}} \quad (7)$$

The $Y_I\%$ was calculated from:

$$Y_I\% = \frac{R_{ct} - R_{ct}^*}{R_{ct}} \times 100 \quad (8)$$

where R_{ct} and R_{ct}^* are the charge-transfer resistances with and without the inhibitors, respectively.

Data in Table (5) show that; the R_s values are very small compared to the R_{ct} values. Also; the R_{ct} values increase and the calculated C_{dl} values decrease by increasing the inhibitor concentrations, which causes an increase of θ and Y_I . The high R_{ct} values are generally associated with slower corroding system [Bosch *et al*, (2001)]. The decrease in the C_{dl} suggests that inhibitors function by adsorption at the metal/solution interface [Lagrenée *et al*, (2002)].

Table(5): EIS data of carbon steel in 2 M HCl and in the presence of different concentrations of inhibitors at 30° C.

Comp.	Conc., (M)	R_s $\Omega \text{ cm}^2$	Y $\mu\Omega^{-1} \text{ s}^n$ cm^{-2}	n	R_{CT} $\Omega \text{ cm}^2$	C_{dl} $\mu\text{F cm}^{-2}$	Θ	% Y_I
Blank	0.0	1,800	135.9	0.923	50.2	177.7	0.53	53.0
CMQ	5.0×10^{-5}	1,719	67.3	0.930	107.0	180.1	0.53	53.0
	1×10^{-4}	1,724	49.3	0.941	171.0	77.8	0.70	70.7
	2.5×10^{-4}	1,788	37.8	0.949	367.0	47.7	0.86	86.3
	5.0×10^{-4}	1,907	37.2	0.919	502.9	40.7	0.90	90.0
	1×10^{-3}	1,777	47.0	0.917	704.0	47.7	0.92	92.3
	2.5×10^{-3}	1,907	42.2	0.919	700.7	40.1	0.93	92.8
MNQ	5.0×10^{-5}	1,990	34.7	1.02	89.95	85.9	0.44	44
	1×10^{-4}	1,887	55.6	0.924	122.9	77.1	0.59	59
	2.5×10^{-4}	1,842	50.6	0.927	100.8	70.0	0.67	67
	5.0×10^{-4}	1,907	48.11	0.921	202.1	61.3	0.75	75
	1×10^{-3}	1,941	43.1	0.921	220.1	54.2	0.85	85
	2.5×10^{-3}	1,07	37.5	0.917	410.0	48.6	0.88	88

The inhibition efficiencies, calculated from EIS results, show the same trend as those obtained from polarization measurements. The difference of inhibition efficiency from two methods may be attributed to the different surface status of the electrode in two measurements. EIS were performed at the rest potential, while in polarization measurements the electrode potential was polarized to high over potential, non-uniform current distributions, resulted from cell geometry, solution conductivity, counter and reference electrode placement, etc., will lead to the difference between the electrode area actually undergoing polarization and the total area [Kelly *et al*, (2002)].

2.3. Electrochemical frequency modulation (EFM) :

EFM is a nondestructive corrosion measurement like EIS; it is a small signal ac technique. Unlike EIS, however, two sine waves (at different frequencies) are applied to the cell simultaneously. The great strength of the EFM is the causality factors which serve as an internal check on the validity of the EFM measurement [Donahue and Nobe, (1965)]. With the causality factors the experimental EFM data can be verified. The results of EFM experiments are a spectrum of current response as a function of frequency. The spectrum is called the intermodulation spectrum. The spectra contain current responses assigned for harmonical and intermodulation current peaks. The larger peaks were used to calculate the corrosion current density (i_{corr}), the Tafel slopes (β_c and β_a) and the causality factors (CF-2 and CF-3). Intermodulation spectra obtained from EFM measurements are presented in Fig.5 for 2 M HCl in absence and presence of 2.5×10^{-3} M of CMQ and MNQ respectively. Similar curves were obtained for other inhibitors (not shown). Table 6 indicated that; the corrosion current densities decrease by increasing the concentrations of the studied inhibitors. The inhibition efficiencies, $Y_{EFM}\%$ calculated from Eq. (9) increase with increasing the studied inhibitor concentrations:

$$Y_{EFM} \% = \frac{i_{corr}^0 - i_{corr}}{i_{corr}^0} \times 100 \quad (9)$$

where: i_{corr}^0 and i_{corr} are corrosion current densities in the absence and presence of inhibitors, respectively.

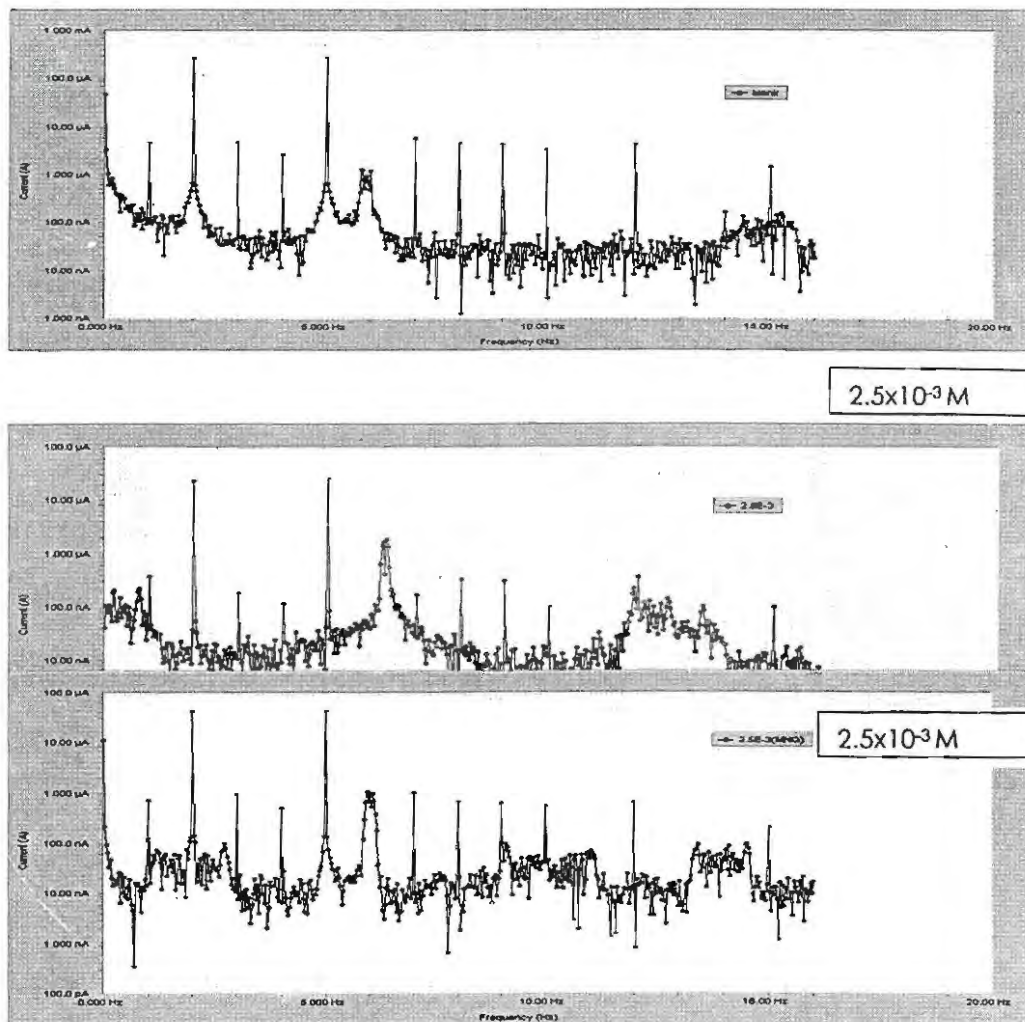


Fig (6) :Intermodulation spectra for carbon steel in 2 M HCl in the absence and presence of 2.5×10^{-3} M CMQ and NMQ

The causality factors in Table 5 are very close to theoretical values which according to the EFM theory [Khamis *et al*, (1991)] should guarantee the validity of Tafel slopes and corrosion current densities.

Table (6): Electrochemical kinetic parameters obtained by EFM technique for C- steel the absence and in presence of various concentrations of inhibitors in 2 M HCl at 30 °C

Compound	Conc., M	j_{corr} μA cm^{-2}	β_c $mVdec^{-1}$	β_a $mVdec^{-1}$	CF- 2	CF- 3	C.R mmy'	% Y_{EFM}
Blank	...	373.5	95.1	85.2	1.78	3.33	166.6	...
CMQ	5×10^{-5}	161.7	101.1	81.9	1.95	3.29	80.1	56.7
	1×10^{-4}	108.3	101.5	83.9	1.89	2.06	53.7	71.0
	2.5×10^{-4}	55.3	99.9	88.5	2.09	2.88	27.4	85.1
	5.0×10^{-4}	42.3	102.3	91.9	2.11	1.79	20.9	88.6
	1×10^{-3}	35.4	99.9	92.1	1.59	3.60	17.6	90.5
	2.5×10^{-3}	32.4	98.3	94.1	2.11	3.04	16.3	91.2
MNQ	5×10^{-5}	210.6	92.1	83.9	2.29	4.6	106.9	43.6
	1×10^{-4}	190.1	101.2	81.3	1.94	2.86	94.2	49.1
	2.5×10^{-4}	102.1	99.9	84.4	1.91	1.42	76.1	58.1
	5.0×10^{-4}	94.2	98.2	86.3	1.94	1.83	46.9	74.6
	1×10^{-3}	87.9	99.1	86.9	1.87	1.19	29.6	83.9
	2.5×10^{-3}	49.1	97.2	90.9	1.80	1.91	26.3	86.7

2.4. Adsorption isotherm :

The mode and extent of the interaction between inhibitor and the iron surface can be studied by applying adsorption isotherms. The degree of surface coverage, θ , at different inhibitor concentrations in 2 M HCl was evaluated from weight loss measurements ($\theta = WE/100$) and is given in Table 2. The fitting to the Langmuir isotherm is shown by plotting C/θ versus C Fig. (7) according to the following equation [Zhao, and Mu, (1999); Chakrabarty et al, (1983)]:

$$C/\theta = 1/K + C \quad (10)$$

$$KC = 1/55.5 \exp(-\Delta G_{ads}^{\circ}) \quad (11)$$

where C is the inhibitor concentration, θ is the fraction of the surface coverage, K is the modified adsorption equilibrium constant which can be related to the free energy of adsorption ΔG_{ads}° and 55.5 is the molar concentration of water in $mol L^{-1}$. In this case,

linear plots with high correlation coefficients and slopes of about unity were obtained, indicating that the experimental results fit the Langmuir isotherm. The values of the correlation coefficients, free energy of adsorption (ΔG°_{ads}) and the adsorption equilibrium constants are given in Table (7). The regression coefficient (R^2) is more than 0.99 suggests a good relation between C/Θ and C . The values of ΔG°_{ads} recorded in Table 7 are negative, suggesting the spontaneity of the adsorption process. It is well known that values of ΔG°_{ads} in the order of 20 kJ mol^{-1} or lower indicate a physisorption, while those of order of 40 kJ mol^{-1} or higher involve charge sharing or charge transfer from the inhibitor molecules to the metal surface to form a coordinate type of bond (chemisorption) [Khamis *et al.*, (1991); Donahue, and Nobe, (1965)]. The calculated ΔG°_{ads} values for CMQ and MNQ in 2 M HCl are 35.2 kJ mol^{-1} and 32.4 kJ mol^{-1} , respectively. This indicates that an electrostatic interaction exists (physisorption) between inhibitor and the charged metal surface. The K value for CMQ is larger than its value for compound MNQ, so compound CMQ strongly adsorbed on carbon steel surface than compound MNQ. The lower K values indicate that these compounds are adsorbed physically on carbon steel surface.

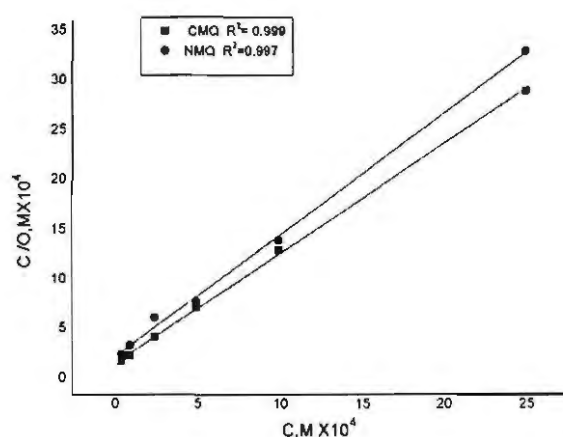


Fig (7) : Langmuir adsorption plots for carbon steel in 2 M HCl containing various concentration of inhibitors

Table (7): Values of adsorption isotherm parameters

Inhibitor	Temp. K	Adsorption isotherm	K M^{-1}	slope	$-\Delta G^{\circ}_{ads}$, kJ mol^{-1}	R^2
CMQ	303	Langmuir	2.4	1.02	35.2	0.9994
MNQ			2.1	1.0	32.4	0.9998

MECHANISM OF CORROSION INHIBITION

The adsorption of quionazolin derivatives can be attributed to the presence of polar unit having atoms of nitrogen and oxygen and aromatic/heterocyclic rings. Therefore, the possible reaction centers are unshared electron pair of hetero-atoms and π -electrons of aromatic ring [Ahmad *et al*, (2010)]. The adsorption and inhibition effect of quionazolin derivatives in 2 M HCl solution can be explained as follows: In aqueous acidic solutions, quionazolin derivatives exist either as neutral molecules or as protonated molecules and may adsorb on the metal/acid solution interface by one and/or more of the following ways: (i) electrostatic interaction of protonated molecules with already adsorbed chloride ions, (ii) donor-acceptor interactions between the π -electrons of aromatic ring and vacant d orbital of surface iron atoms, (iii) interaction between unshared electron pairs of hetero-atoms and vacant d-orbital of iron surface atoms. In general, two modes of adsorption are considered on the metal surface in acid media. In the first mode, the neutral molecules may be adsorbed on the surface of carbon steel through the chemisorption mechanism, involving the displacement of water molecules from the carbon steel surface and the sharing electrons between the hetero-atoms and iron. The inhibitor molecules can also adsorb on the carbon steel surface on the basis of donor-acceptor interactions between π -electrons of the aromatic ring and vacant d-orbitals of surface iron atoms. In the second mode, since it is well known that the steel surface bears positive charge in acid solution [Singh, and Quraishi, (2010)], so it is difficult for the protonated molecules to approach the positively charged carbon steel surface due to the electrostatic repulsion. Since chloride ions have a smaller degree of hydration, thus they could bring excess negative charges in the vicinity of the interface and favor more adsorption of the positively charged inhibitor molecules, the protonated quionazolin derivatives adsorb through electrostatic interactions between the positively charged molecules and the negatively charged metal surface. Thus there is a synergism between adsorbed Cl^- ions and protonated quionazolin derivatives. Thus we can conclude that inhibition of carbon steel corrosion in 2 M HCl is mainly due to electrostatic interaction. The decrease in inhibition efficiency with rise in temperature supports electrostatic interaction.

Variation in structure of inhibitors molecules takes place through the phenyl group. Hence, the inhibition efficiency depends on this part of the molecule. Investigated quionazolin derivatives have an electron-withdrawing groups such as $-\text{Cl}$ and $-\text{NO}_2$ which may decrease the electron density on molecules. The order of decreasing inhibition efficiency of these compounds is: $-\text{Cl} > -\text{NO}_2$. This order of decreased inhibition efficiency of these additives can be accounted for in terms of polar effect [Hammett, (1940)] of the *p*-substituent's on phenyl group. Compound CMQ is the most efficient inhibitor, because the presence of withdrawing group ($-\text{Cl}$) in *p*-position with $\sigma = +0.23$ (Hammett constant) [51] and Cl atom has dual effect (withdrawing group and in the same time may act as center of adsorption). Compound NMQ comes after compound CMQ in inhibition efficiency, because it has $\sigma = +0.78$. So, the order of inhibition depends on the magnitude of their withdrawing character.

CONCLUSIONS

- The quionazolin derivatives inhibit the corrosion of carbon steel in 2 M HCl.
- The inhibition is due to adsorption of the inhibitor molecules on the carbon steel surface by blocking its active sites.
- Adsorption of quionazolin derivatives fits Langmuir isotherm isotherm.
- Results obtained from weight loss, DC polarization, AC impedance and EFM techniques are reasonably in good agreement and show increased inhibitor efficiency with increasing inhibitor concentration.
- Polarization data showed that the used inhibitors act as mixed-type inhibitor in 2 M HCl.

REFERENCES

- Abboud Y., Abourriche A., Saffag T., Berrada M., Charrouf M., Bennamara A., Al Himidi N., and Hannache H., *Mater. Chem.phy.*105 (2007) 1-5.
- Abd El-Maksoud S.A., Fouda A.S., *Mater.Chem.phys.*93(2005) 84-90
- Abdallah M., Helal E. A. and Fouda A. S., *Corros. Sci.*, 48 (2006) 1639-1654.
- Ahamad I., Prasad R., and Quraishi M.A., *Corros. Sci.*, 52 (2010) 3033.
- Ajmal M., Mideen A.S., and Quraishi M.A., *Corros.Sci.*, 36(1994)79.
- Akust A.A., Lorenz W.J.and Mansfeld F., *Corros.Sci.*, 22(1982) 611.
- Ashassi-sorkhabi H., Magidi M.R., and Seyyedi K., *Appt. Surf. Sci.*, 225 (2004)176-185
- Avci G., *Colloids Surf. A* 317 (2008)730-736
- Benali O., Larabi L., Traisnel M, Gengembra L., Harwk Y., *Appi. Surf. Sci* 253(2007)6130-6139.
- Bentiss F., Lebrini M., and Lagrenee M., *Corros. Sci.*47(2005) 2915-2931.
- Bockris JO'M., and Yang B., *J.Electrochem.Soc.*, 138(1991) 2237.
- Bosch R.W., Hubrecht J., Bogaerts W.F. and Syrett B.C., *Corrosion*, 57 (2001) 60.
- Chakrabarty C., Singh M.M., Yadav P.N.S., and Agarwal C.V., *Trans.SAEST*, 18(1983)15.

Deyab M.A., *Corros. Sci.* 49(2007) 2315-2328

Donahue F.M. and Nobe K., *J. Electrochem. Soc.* 112 (1965) 886.

Donahue F.M., and Nobe K., *J. Electrochem. Soc.*, 112(1965)886.

El Achouri M., Kertit S., Gouttaya H.M., Nciri B., Bensouda Y., Perez L., Infante M.R. and Elkacemi K., *Prog. Org. Coat.*, 43 (2001) 267.

Fouda A. S., Al-Sarawy A. A. and El-Katori E. E., *Desalination J.*, 201 (2006) 1-13.

Fouda A. S., Al-Sarawy A. A. and El-Katori E. E., *Chem. Paper*, 60(1) (2006) 5-9.

Gao, X., Cai X., Yan K., Song B., and Gao L., *Chem Z.*, *Molecules*, 12(12)(2007) 2621-2642.

Growcock F.B. and Jasinski J.H., *J. Electrochem. Soc.*, 136 (1989) 2310

Hammett L.P., "Physical Organic Chemistry" McGraw-Hill Book Co., N.Y. (1940).

Hsu C.H., and Mansfeld F., *Corrosion* 57 (2001) 747.

Jovancicevic V., Yang B. and Bockris JO'M., *J. Electrochem. Soc.*, 135(1989) 94

Kelly R.G., Scully J.R., Shoesmith D.W., and Buchheit R.G., *Electrochemical Techniques in Corrosion Science and Engineering*, Marcel Dekker, Inc., New York, 2002. p. 148.

Khaled K.F., *Electrochim. Acta* 48 (2003)2493-2503

Khaled K.F., *Electrochim. Acta*, 48 (2003) 2493.

Khaled K.F., *Mater. Chem. phys.* 122(2008) 290-300

Khalifa, M.A., El-Batouti M., Mhgoub F., Bakr A., Aknish, *Mater. Corrps.* 54(2003)251-258.

Khamis E., Bellucci F., Latanision R.M. and El-Ashry E.S.H., *Corrosion*, 47(1991)677.

Khamis E., Bellucci F., Latanision R.M., and El-Ashry E.S.H., *Corrosion* 47 (1991) 677.

Lagrene M., Mernari B., Bouanis B., Traisnel M. and Bentiss F., *Corros. Sci.*, 44 (2002) 573.

- Lebrini M., Lagrenée M., Traisnel M., Gengembre L., Vezin H. and Bentiss F., *Appl. Surf. Sci.*, 253 (2007) 9267
- Machnikova E., Pazderova M., Bazzaoui M. and Hackerman N., *Surf. Coat. Technol.*, 202 (2008) 1543.
- Machnikova E., Whitmire K.H. and Hackerman N., *Electrochim. Acta* 53(2008) 6024-6032
- Mehaute A.H., and Grepy G., *Solid State Ionics* 9–10 (1983) 17.
- Migahed M.A., and Nasser I.F., *Electrochim. Acta* 53 (2008) 2877- 2882
- Noot E.A and Al-Moubaraki A.H., *Mater. Chem.phys.*110(2008)145-154.
- Pillali K.C., and Narayan R., *Corros.Sci.*, 23(1985)151
- Popova A., Chistov M., Raicheva S. and Sokolova E., *Corros. Sci* 46(2004)1333-1350.
- Rammet U. and Reinhart G., *Corros. Sci.*, 27 (1987) 373.
- Singh A.K., and Quraishi M.A., *Corros. Sci.*, 52 (2010) 1529.
- Tadros A.B., and Abdel-Naby B.A., *J.Electroanal.Chem.*, 224(1988) 433.
- Uhera J., and Aramaki K., *J.Electrochem.Soc.*, 138(1991)3245.
- Zhao T.P., and Mu G.N., *Corrosion Sci.*, 41(1999)1937.

المخلص العربي

مثبطات تآكل الصلب الكربوني في الوسط الحامضي

ا. د. عبد العزيز السيد فودة - ا. د. يحيى عبد اللطيف العواضي - ا. د. هانم عبد الرسول مصطفى وصلاح احمد محمد حبوبة

التآكل هو المشكلة الرئيسية التي تهدد فترة عمر صلاحية المعدن للاستخدام وفهم ميكانيكية التآكل يمكننا من ايجاد حل لمشاكل التآكل الحالية ومنع المشاكل المستقبلية وهذا البحث يناقش تآكل الصلب الكربوني في حامض الهيدروكلوريك وكيفية حمايته.

تم مناقشة التركيب الكيميائي لمركبات الكينازولين وتأثيرها على كفاءة التثبيط ولوحظ أن كفاءة تثبيط المركبات يعتمد على الشكل الفراغي للمركبات والمراكز النشطة الموجودة في المركبات التي الكثافة الالكترونية على سطح الصلب الكربوني

وتمت الدراسات باستخدام الطرق التالية :

(طريقة الفقد في الوزن والاستقطاب البوتنشو ديناميكي والمعاوقة كهربية والتيار المتردد والتردد الكهركيميائي المعدل)

وخلص القول أن القياسات المستخدمة تؤيد افتراض أن تثبيط التآكل يتم عن طريق ادمصاص المثبطات على سطح الصلب الكربوني والاتفاق بين وسائل القياسات المختلفة في ترتيب كفاءة المثبطات المستخدمة وهذا يدل على صحة النتائج التي تم الحصول عليها.

